Molten-Metal Electrodes for Solid Oxide Fuel Cells

A. Jayakumar, J. M. Vohs, and R. J. Gorte*

Department of Chemical and Biomolecular Engineering, University of Pennsylvania, Philadelphia, Pennsylvania 19104

Molten In, Pb, and Sb were examined as anodes in solid oxide fuel cells (SOFC) that operate between 973 and 1173 K. The results for these metals were compared with those reported previously for molten Sn electrodes. Cells were operated under "battery" conditions, with dry He or N_2 flow in the anode compartment, to characterize the electrochemical oxidation of the metals at the yttria-stabilized zirconia (YSZ)-electrolyte interface. In most cases, the open-circuit voltages (OCVs) were close to that based on equilibrium between the metals and their oxides. With Sn and In, the cell impedances increased dramatically at all temperatures after drawing current due to formation of insulating, oxide barriers at the electrolyte interface. Similar results were observed for Pb at 973 and 1073 K, but the impedance remained low even after PbO formation at 1173 K because this is above the melting temperature of PbO. Similarly, the impedances of molten Sb electrodes at 973 K were low and unaffected by current flow because of the low melting temperature of Sb_2O_3. The potential of using molten-metal electrodes for direct-carbon fuel cells and for energy-storage systems is discussed.

Introduction

There has recently been significant interest in development of fuel cells that can generate power from coal electrochemically.[1−6] In principle, such fuel cells could provide electricity at much higher efficiency than is possible using combustion processes. Furthermore, with fuel cells based on electrolytes that are oxygen-ion conductors, the CO_2 would be produced in a concentrated form, making it much easier to employ sequestration strategies for when CO_2 emissions become regulated. Although most approaches to using coal in fuel cells involve some kind of gasification followed by steam reforming to produce syngas that would then be used by the fuel cell,[2] a process that could utilize the carbon directly would have the advantage of process simplicity.

One of the more interesting schemes for the development of direct-carbon fuel cells (DCFC) involves the use of solid oxide fuel cells (SOFC) with molten-metal anodes.[7−9] In this approach, oxygen from the electrolyte is transferred to the molten metal to form the metal oxide via reaction 1.

$$M + nO^{2-} = MO_n + 2ne^- \quad (1)$$

The metal oxide is then reduced by the fuel, either in the anode compartment itself or by removing the oxygen-saturated metal and reducing it in a separate reactor. Implementation of this strategy is under way with molten Sn anodes.[4−6] However, there is very little published data available on the factors that limit the performance of SOFC with molten-Sn electrodes, and the data that is available suggests that the cells exhibit relatively high impedances, requiring that they be operated at temperatures above 1273 K.[9] Therefore, our group has been investigating SOFC with molten-metal anodes to better understand the electrochemical reactions.

In previous work, we studied fuel cells with molten Sn and molten Bi anodes.[7] The cells were studied in the "battery" mode, operating the cells with oxidation of the molten metal in the absence of fuel to focus on Reaction 1. With Sn, the open-circuit voltage (OCV) was ∼0.93 V at 973 K, close to the equilibrium Nernst potential for oxidation of Sn. This potential, which is roughly 0.1 V lower than the equilibrium value for carbon oxidation to CO_2, is nearly ideal for a DCFC because it implies reduction of the oxide by carbon should be thermodynamically spontaneous while still allowing the fuel cell to produce electrons at a high enough potential for a high system efficiency. The problem with Sn is that oxygen solubility in the metal is very low. Therefore, oxidation at the electrolyte surface causes the formation of an insulating, SnO_2 layer at the electrolyte interface, leading to large increases in the cell impedance after transfer of just a few Coulombs per square centimeter of charge. With molten Bi, the oxygen solubility is similarly low, but the oxide is a good ion conductor, so that there is no increase in impedance, even after transfer of many Coulombs per square centimeter. The problem with Bi is that its OCV is only 0.48 V. It is not yet clear whether the presence of fuel in the molten Bi could reduce the oxide at a sufficient rate to prevent reaction 1 from reaching equilibrium so that a cell with a molten-Bi anode could operate at a higher potential; however, this would certainly not allow the oxidized Bi to be reduced in a reactor separated from the anode compartment of the fuel cell.

In the present paper, we present and discuss results from the study of fuel cells based on several additional molten-metal anodes: In, Pb, and Sb. The melting temperatures of these metals are 430, 601, and 904 K, respectively. Molten In is similar to Sn in that its oxide has a low solubility in the metal and a very high melting temperature, making it useful for determining whether the effects observed with molten Sn anodes are generally applicable to metals and oxides with these properties. Pb and Sb are of interest because their oxides have relatively low melting temperatures, 1161 K for PbO and 929 K for Sb_2O_3. This would allow the oxides to be removed from anode compartment as well as provide a mechanism for removing the oxide layer from the electrolyte interface.

In this study, we will show that the melting temperature of the oxide is, indeed, important in determining the performance of the electrodes. The results for the $Sb-Sb_2O_3$ system are particularly interesting, especially for energy-storage applications.

Experimental Section

The experimental techniques were essentially the same as those used in our previous study of molten Sn and Bi anodes.[7]

* To whom correspondence should be addressed. E-mail: gorte@seas.upenn.edu.

10.1021/ie100457t
Published on Web 05/26/2010

The electrolyte and cathode of the fuel cells used in this study were prepared from a dense YSZ wafer with a porous YSZ layer on one side that was fabricated by tape-casting methods.[10−13] The active component of the cathode was added to the porous YSZ side by infiltration with an aqueous solution of $La(NO_3)_3$, $Fe(NO_3)_3$, and $Sr(NO_3)_2$, together with citric acid, to produce a 40 wt % $La_{0.8}Sr_{0.2}FeO_3$/yttria-stabilized zirconia (LSF-YSZ) composite.[12,13] The final calcination temperature for the cathode composite was 1123 K. For the present study, the dense electrolyte layers were ∼600 μm thick, whereas the porous layers used in making the cathode composites were 50 μm thick. Both the dense and the porous layers were circular, but the diameter of the dense layers was 1 cm and the diameter of the porous layer was 0.67 cm.

After preparation of the cathode, the cell was mounted onto an alumina tube using a ceramic adhesive (Aremco Ceramabond 522). The tube was in turn mounted vertically so the molten metal could be kept in contact with the YSZ electrolyte by gravity. Current collection at the anode was accomplished using a ceramic wafer of $La_{0.3}Sr_{0.7}TiO_3$ (LST), suspended in the molten metal above the electrolyte. An alumina tube with Ag wire in the center was pasted onto the LST wafer. Since molten metals tend to "ball up" on the YSZ electrolyte surface, the LST wafer was also used to press the metals onto the electrolyte surface. For the present study, 1200 mg of either In (Alfa-Aesar), Pb (Alfa-Aesar), or Sb (Sigma Aldrich) was added to the anode compartment. On the basis of the density of metals and the inner diameter of the tube used for the anode compartment, this resulted in metal layers that were ∼2.0−2.5 mm thick.

For electrochemical characterization, the cathode was held in air, and a gas flow was maintained over the anode. Because we were interested in reaction 1, all of the experiments in the present study were conducted in the battery mode, in which the gas above the anode was either dry He or N_2; however, the anodes were first reduced in humidified (3% H_2O) H_2 for at least 30 min to reduce the molten metals, after which the H_2 was flushed from the anode by flowing He or N_2. Impedance spectra and voltage−current ($V-i$) polarization curves were measured using a Gamry Instruments potentiostat. Impedance spectra were measured galvanostatically at various currents in the frequency range of 300 kHz to 0.1 Hz, with a 1 mA ac perturbation. We used the average of the anode and cathode diameters to calculate the effective electrode area, which was then used to normalize the current densities. Because the ionic conductivity of YSZ is well-known[14] and the impedance of the infiltrated LSF-YSZ cathode has been extensively characterized in previous studies,[12,13] the performance of the molten-metal anodes could be determined by difference.

Results

Although results for molten-Sn anodes have been discussed previously,[7] we present a brief summary here to point out the issues that arise with this material. Figure 1 shows the V-i polarization curves for a cell with a Sn anode at 973 and 1073 K obtained by ramping the voltage from its open-circuit value, to zero volts, and back to the open-circuit potential at 10 mV/s, while measuring the current produced by the cell. The $V-i$ curves show that the OCV for Sn is 0.93 V at these temperatures, close to the theoretical Nernst potential for reaction 1. Although the current initially increases as the voltage decreases due to the increasing overpotentials at the electrodes and electrolyte, the current goes through a maximum and then decreases due to formation of the SnO_2 layer at the electrolyte interface. When the cell potential is allowed to again increase, the current density

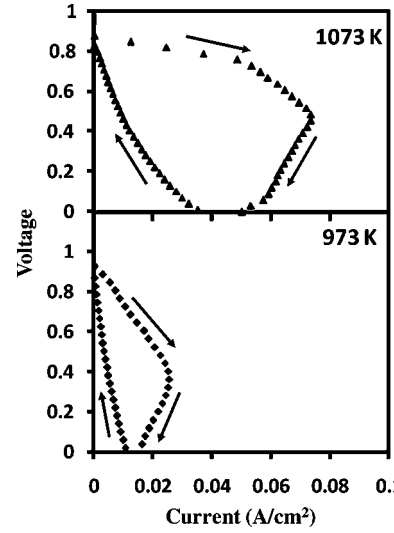

Figure 1. $V-i$ polarization curve for a cell with molten Sn as the anode at 973 and 1073 K. After reduction of the Sn in humidified H_2, the anode compartment was exposed to dry, flowing He while ramping the voltage from open circuit and back at 10 mV/s.

remains low due to the insulating oxide barrier.[7] The original cell performance could only be restored by again flowing H_2 into the anode compartment resulting in reduction of the SnO_2 layer. Impedance data presented previously demonstrated that the ohmic resistance of the cell remained unchanged after completing the voltage-current cycle but that the nonohmic impedance increased dramatically because of the barrier to diffusion of the oxide ions from the electrolyte. The thickness of the oxide layer can be calculated from the Coulombs of charge that was transferred at the time of maximum current, using the bulk density of SnO_2. These values are 0.47 μm at 973 K and 0.80 μm at 1073 K. These values are somewhat lower than that measured by scanning electron microscopy, suggesting that the oxide films are not completely dense.

A similar set of data was obtained for the cell with the molten-In anode, with the $V-i$ polarization curves reported in Figure 2. After reducing the anodes in flowing H_2, the initial OCV was 1.01 V at 973 K, but decreased slightly with temperature, in agreement with the theoretical Nernst potential. As with the molten-Sn anodes, the current went through a maximum when the voltage was ramped down from OCV to zero and back at 10 mV/s. With In at 1173 K, the OCV also did not quite return to the Nernst potential after the voltage-current cycle, possibly because of current leakage and the large internal losses associated with the oxide layer. Using the same calculation as that used with Sn to estimate the characteristic oxide film thicknesses, we estimated the layers to be 0.41, 0.89, and 2.0 μm at 973, 1073, and 1173 K, respectively. It is interesting that the oxide layer can be significantly thicker at the higher temperatures before the cell impedance increases dramatically. Certainly, part of the reason for this is the increased diffusivity of oxygen with increasing temperature. However, the result may also indicate changes in the way the film grows. For example, there may be more extensive dendrites of the oxide extending into the molten In at the higher temperatures.

The Cole−Cole plots of the cell impedances for the cell with molten In, measured at OCV and 1073 K before and after completing the voltage scan, are shown in Figure 3. These impedance data show that the ohmic contribution to the impedance, ∼1.2 Ω cm^2, is unchanged after passing current and is close to the expected value of 1.4 Ω cm^2 based on the reported conductivity of YSZ at 1073 K, 0.0428 S/cm,[14] and the thickness of the

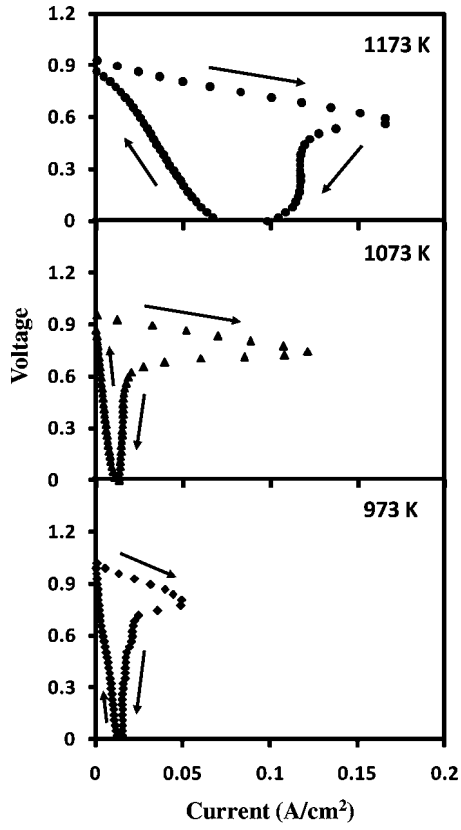

Figure 2. $V-i$ polarization curve for a cell with molten In as the anode at 973, 1073, and 1173 K. After reduction of the In in humidified H_2, the anode compartment was exposed to dry, flowing N_2 while ramping the voltage from open circuit and back at 10 mV/s.

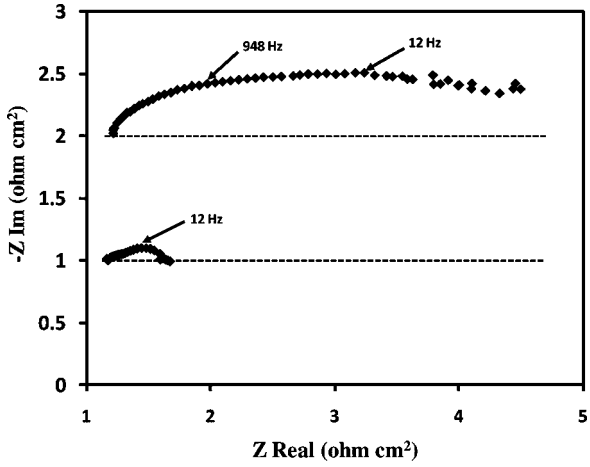

Figure 3. Impedance data for the cell with the molten In anode at 1073 K, corresponding to the $V-i$ polarization data in Figure 2. The bottom curve is the Cole−Cole plot obtained near open circuit immediately after reduction of the In, while the top curve was obtained after completing the ramp from open circuit to 0 V and back.

electrolyte, 600 μm. The change that occurs after passing current through the cell is mainly in the nonohmic losses, determined from the length of the arc under the Cole−Cole plot, which increases from ~0.4 Ω cm^2 to greater than 3 Ω cm^2. At 1073 K, the impedance of the LSF-YSZ cathode is less than 0.1 Ω cm^2,[12,13] so that most of the nonohmic losses arise from the anode, even before passing current through the cell. After the voltage cycle, most of the losses are clearly associated with an In_2O_3 barrier at the electrolyte interface. The peak frequency of approximately 12 Hz in the deactivated cell is also characteristic of a diffusion

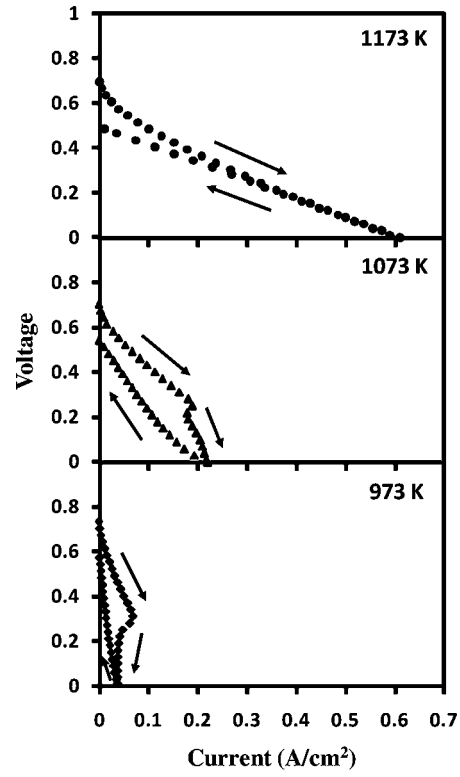

Figure 4. $V-i$ polarization curve for a cell with molten Pb as the anode at 973, 1073, and 1173 K. After reduction of the Pb in humidified H_2, the anode compartment was exposed to dry, flowing N_2 while ramping the voltage from open circuit and back at 10 mV/s.

process. Experiments performed at 973 and 1173 K gave results that were qualitatively similar.

It seems apparent that performance improvements with molten-metal anodes require minimizing the losses associated with the oxide barrier formed at the anode−electrolyte interface. In a previous paper, we demonstrated that the effects of the oxide barrier were minimal with Bi due to the fact that its oxide is a good ion conductor. An alternate approach to avoiding losses associated with oxide formation at the electrolyte is to use metals that have oxides with low melting temperatures, such as Pb and Sb, whose oxides melt at 1161 and 929 K respectively. The $V-i$ polarization curves for Pb, obtained using the same voltage−current ramps as that used with In, are shown in Figure 4 at 973, 1073, and 1173 K. The initial OCV of the freshly reduced cell were slightly higher than the expected Nernst potentials at the three operating temperatures: 0.60, 0.55, and 0.5 V. This suggests that some H_2 remained in the anode compartment after flushing with inert gases, perhaps dissolved in the molten Pb. For operation at temperatures below the melting point of PbO, the voltage−current characteristics are similar to that observed with In and Sn. The $V-i$ curves change after current has passed through the cell. At 1173 K, however, the only effect on the $V-i$ polarization curve due to passing current is that it becomes a straight line passing through the Nernst potential.

The impedance data in Figure 5 more clearly demonstrate the effect that operation above the melting temperature of PbO has on cell performance. At 1073 K, the initial impedance at open circuit shows the ohmic losses are 1.23 Ω cm^2 and the nonohmic losses are 0.17 Ω cm^2. As discussed in the results for In, the ohmic losses are close to that expected for the YSZ electrolyte, and the nonohmic losses are very low. After completing the voltage−current cycle, the OCV impedance data show that the ohmic losses are unaffected but the nonohmic

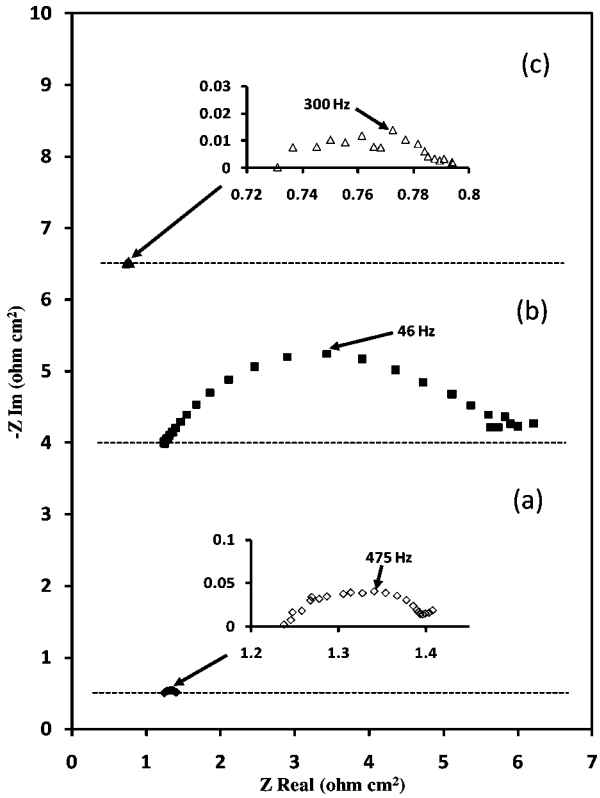

Figure 5. Impedance data for the cell with the molten Pb anode, corresponding to the $V-i$ polarization data in Figure 4. Curve a is the Cole−Cole plot obtained near open circuit at 1073 K immediately after reduction of the Pb; curve b, above it, was obtained after completing the ramp from open circuit to 0 V and back. Curve c was obtained on the same cell at 1173 K, near open circuit, after completing the voltage ramp.

losses are now unacceptably high, 5 Ω cm^2. By contrast, the impedance obtained at 1173 K was independent of current density or voltage−current cycling. The ohmic and nonohmic losses at this temperature were 0.73 and 0.06 Ω cm^2, respectively. Obviously, the OCV for Pb at 1173 K is still undesirably low, but the losses associated with electrode performance are impressively small.

To confirm that performance can be very good when using a molten-metal anode for which the oxide has a low melting temperature, we performed similar experiments with Sb. Because the seals in our experimental apparatus were inadequate for preventing Sb_2O_3 from leaking through and breaking the electrical connections (The Ceramabond appears to be porous to Sb_2O_3.), we were able to obtain only a limited set of data at 973 K with our present apparatus; however, these initial results were promising. At 973 K, the $V-i$ polarization data in Figure 6 are linear, with an OCV of 0.75 V, equal to the Nernst potential for Sb. There were no changes after allowing current to flow for several hours at short circuit. The impedance results in Figure 7 are consistent with this. The ohmic losses in this cell, 4.6 Ω cm^2, were higher than the expected value for the 600 μm electrolyte, 3.2 Ω cm^2, possibly due to poor electrical connections; but nonohmic losses, ~0.6 Ω cm^2, were reasonably low.

Discussion

The performance data for anodes based on molten Pb and molten Sb for operation above the melting temperature of their oxides are most promising and demonstrate that the impedance for this type of electrode can be very good. So long as one can avoid the formation of oxide barriers, the impedance associated

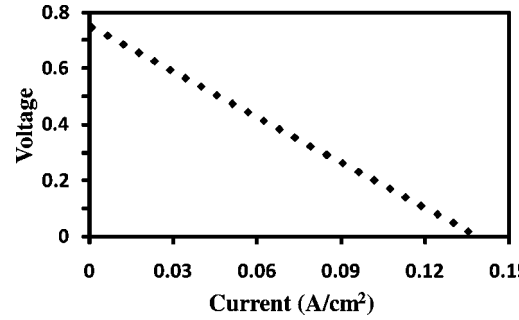

Figure 6. $V-i$ polarization curve for the cell with the molten Sb anode at 973 K. After reduction of the Sb in humidified H_2, the anode compartment was exposed to dry, flowing N_2.

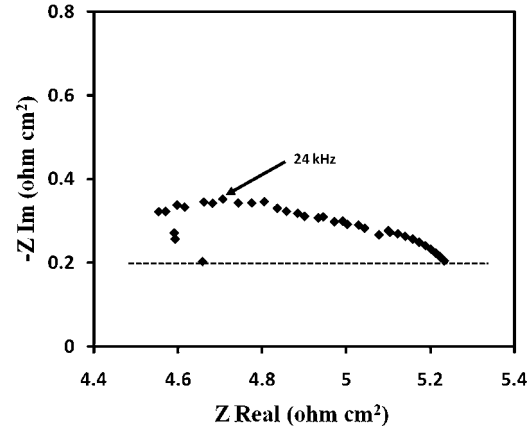

Figure 7. Impedance data for the cell with the molten Sb anode at 973 K, corresponding to the data in Figure 6.

with oxygen transfer at the metal−electrolyte interface is very low so that high cell efficiencies could be expected. When both the metal and the oxide exist in the molten state, it is also easy to transport oxygen into a separate reactor for reduction by carbon.

One important issue is the open-circuit potential. For a fuel cell in which the electrons ultimately come from oxidation of carbon, anything below approximately 1.0 V will result in an energy loss. Obviously, the potential associated with equilibrium between a metal and its oxide is a fundamental property that is not adjustable. However, if the chemical potential of oxygen in the molten metal can be kept below that required to form the oxide, such as might be the case when fuel is present with the metal in the anode compartment, then the theoretical OCV would be determined by the thermodynamics of the fuel oxidation reaction. This is obviously the situation for normal SOFC operation with Ni-based anodes, for which great care is taken to maintain the $P(O_2)$ below that at which Ni is in equilibrium with NiO.

Furthermore, the relatively low Nernst potential associated with oxidation of molten Sb would not be a problem for energy-storage systems, for which the oxide would be reduced to the metal by electrolysis during times of excess energy and the metal would be used to generate power during times when energy was needed. Indeed, the Sb−Sb_2O_3 system appears to have many attractive features for this application, given that the volumetric energy density of the metal would be relatively high as compared with that of H_2, which would be produced by normal steam electrolysis. In reversible H_2-H_2O fuel cells, there would also likely be an energy cost associated with pumping the H_2 to higher pressures.

Since there have been few studies of molten-metal electrodes, there is still much that is not known about these systems. In addition to the performance issues we have investigated here, relatively little is known about the reactivity of these materials with YSZ after long times at elevated temperatures. As was clear from our results with Sb, seals may well be a serious problem. Finally, the molten metals will produce an extremely corrosive environment. Still, the molten-metal electrodes are very interesting, and these systems could have applications in direct-carbon fuel cells and in energy-storage systems.

Conclusions

The impedance of molten-metal electrodes appears to be limited by formation of an oxide barrier at the electrode−electrolyte interface. By working at temperatures above the melting temperatures of both the metal and its oxide, it is possible to minimize the effect of oxide formation and achieve excellent electrode performance. These systems may have application in direct-carbon fuel cells and energy-storage systems.

Acknowledgment

This work was supported as part of the Catalysis Center for Energy Innovation, an Energy Frontier Research Center funded by the U.S. Department of Energy, Office of Science, Office of Basic Energy Sciences under Award no. DE-SC0001004.

Literature Cited

(1) Cao, D. X.; Sun, Y.; Wang, G. L. Direct Carbon Fuel Cell: Fundamentals and Recent Developments. *J. Power Sources* **2007**, *167*, 250–257.

(2) Li, S.; Lee, A. C.; Mitchell, R. E.; Gür, T. M. Direct Carbon Conversion in a Helium Fluidized Bed Fuel Cell. *Solid State Ionics* **2008**, *172*, 1549–1552.

(3) Nabae, Y.; Pointon, K. D.; Irvine, J. T. S. Electrochemical Oxidation of Solid Carbon in Hybrid DCFC with Solid Oxide and Molten Carbonate Binary Electrolyte. *Energy Environ. Sci.* **2008**, *1*, 148–155.

(4) Tao, T.; Bateman, L.; Bentley, J.; Slaney, M. Liquid Tin Anode Solid Oxide Fuel Cell for Direct Carbonaceous Fuel Conversion. *ECS Trans.* **2007**, *5*, 463–472.

(5) Tao, T.; Slaney, M.; Bateman, L.; Bentley, J. Anode Polarization in Liquid Tin Anode Solid Oxide Fuel Cell. *ECS Trans.* **2007**, *7*, 1389–1397.

(6) Program on Technology Innovation: Systems Assessment of Direct Carbon Fuel Cells Technology. Electric Power Research Report Number 1016170, EPRI, Alto, CA, 2008.

(7) Jayakumar, A.; Lee, S.; Hornes, A.; Vohs, J. M.; Gorte, R. J. A Comparison of Molten Sn and Bi for Solid Oxide Fuel Cell Anodes. *J. Electrochem. Soc.* **2010**, *157*, B365–B369.

(8) Pati, S.; Yoon, K. J.; Gopalan, S.; Pal, U. B. Hydrogen Production Using Solid Oxide Membrane Electrolyzer with Solid Carbon Reductant in Liquid Metal Anode. *J. Electrochem. Soc.* **2009**, *156*, B1067–B1077.

(9) McPhee, W. A. G.; Boucher, M.; Stuart, J.; Parnas, R. S.; Koslowske, M.; Tao, T.; Wilhite, B. A. Demonstration of a Liquid-Tin Anode Solid-Oxide Fuel Cell (LTA-SOFC) Operating from Biodiesel Fuel. *Energy Fuels* **2009**, *23*, 5036–5041.

(10) Vohs, J. M.; Gorte, R. J. High-Performance SOFC Cathodes Prepared by Infiltration. *Adv. Mater.* **2009**, *21*, 943–956.

(11) Park, S.; Gorte, R. J.; Vohs, J. M. Tape Cast Solid Oxide Fuel Cells for the Direct Oxidation of Hydrocarbons. *J. Electrochem. Soc.* **2001**, *148*, A443–A447.

(12) Huang, Y. Y; Vohs, J. M.; Gorte, R. J. Fabrication of Sr-Doped $LaFeO_3$-YSZ Composite Cathodes. *J. Electrochem. Soc.* **2004**, *151*, A646–A651.

(13) Wang, W.; Gross, M. D.; Vohs, J. M.; Gorte, R. J. The Stability of LSF-YSZ Electrodes Prepared by Infiltration. *J. Electrochem. Soc.* **2007**, *154*, B439–B445.

(14) Sasaki, K.; Maier, J. Re-analysis of defect Equilibria and Transport Parameters in Y_2O_3-Stabilized ZrO_2 Using EPR and Optical Relaxation. *Solid State Ionics* **2000**, *134*, 303–321.

Received for review March 01, 2010
Revised manuscript received May 7, 2010
Accepted May 19, 2010

IE100457T